

1 **Horizontal and vertical food web structure drives trace element trophic transfer in Terra**  
2 **Nova Bay, Antarctica**

3

4 Geraldina Signa <sup>a,b</sup>, Edoardo Calizza <sup>b,c,\*</sup>, Maria Letizia Costantini <sup>b,c</sup>, Cecilia Tramati <sup>a</sup>, Simona  
5 Sporta Caputi <sup>c</sup>, Antonio Mazzola <sup>a,b</sup>, Loreto Rossi <sup>b,c</sup>, Salvatrice Vizzini <sup>a,b</sup>

6 <sup>a</sup> Department of Earth and Marine Sciences, University of Palermo, via Archirafi 18, 90123  
7 Palermo, Italy

8 <sup>b</sup> CoNISMa, Consorzio Nazionale Interuniversitario per le Scienze del Mare, Piazzale Flaminio 9,  
9 00196 Rome, Italy

10 <sup>c</sup> Department of Environmental Biology, Sapienza University of Rome, Via dei Sardi 70, 00185  
11 Rome, Italy

12 \* Corresponding author: Edoardo Calizza; edoardo.calizza@uniroma1.it

13

14 **Abstract**

15 Despite in the last decades a vast amount of literature has focused on trace element (TE)  
16 contamination in Antarctica, the assessment of the main pathways driving TE transfer to the biota  
17 is still an overlooked issue. This limits the ability to predict how variations in sea-ice dynamics and  
18 productivity due to climate change will affect TE allocation in food webs. Here, food web structure  
19 of Tethys Bay (Terra Nova Bay, Ross Sea, Antarctica) was first characterised using carbon and  
20 nitrogen stable isotopes ( $\delta^{13}\text{C}$ ,  $\delta^{15}\text{N}$ ) of organic matter sources (sediment and planktonic, benthic  
21 and sympagic primary producers) and consumers (zooplankton, benthic invertebrates and  
22 vertebrates). Then, relationships between TEs (Cd, Cr, Co, Cu, Hg, Ni, Pb and V) and stable  
23 isotopes were assessed in order to evaluate if and how horizontal (organic matter pathways) and  
24 vertical (trophic position) food web features influence TE transfer to the biota. Regressions  
25 between  $\log[\text{TE}]$  and  $\delta^{13}\text{C}$  revealed that the sympagic pathway drives accumulation of V in primary

26 consumers and of Cd and Hg in secondary consumers, and that a coupled benthic/planktonic  
27 pathway drives Pb transfer to all consumers. Regressions between  $\log[\text{TE}]$  and  $\delta^{15}\text{N}$  showed that  
28 only Hg biomagnifies across trophic levels, while all the others TEs showed a biodilution pattern,  
29 consistent with patterns observed in temperate food webs. Although the Cd behavior needs further  
30 investigations, the present findings provide new insights about the role of basal sources in the  
31 transfer of TEs in polar systems, especially important nowadays in light of the forecasted trophic  
32 changes potentially resulting from future climate change-induced modification of sea-ice dynamics.

33

34 **Capsule** : Depiction of trace element transfer in the Antarctic food web highlighted an important  
35 role of both sympagic and phytoplanktonic pathways, suggesting that forecasted modification of  
36 sea-ice dynamics due to climate change may alter contaminant accumulation and biomagnification  
37 patterns.

38

### 39 **Keywords**

40 metal; stable isotopes; sympagic algae; biomagnification; polar

41

## 42 **1. Introduction**

43 Despite Antarctica is a remote area, commonly seen as an undisturbed and pristine environment,  
44 many scientific researches revealed that contamination is an important issue, due to a combination  
45 of natural and anthropogenic processes. In the last decades, much research on trace element (TE)  
46 contamination has been carried out in Antarctica. Atmospheric deposition of airborne particles from  
47 other areas in the Southern Hemisphere was identified as the main process that contributes to the  
48 high levels of many trace elements (i.e. Cd, Cr, Cu, Hg, Ni, Pb, V and Zn) found in the surface  
49 ocean, snow and pack-ice (Bargagli, 2008; Bargagli et al., 2005; Sañudo-Wilhelmy et al., 2002;  
50 Tuohy et al., 2015). Continental runoff, soil leaching and ice-melting further increase dissolved and

51 particulate contaminants into the coastal areas (Negri et al., 2006; Prendez and Carrasco, 2003).  
52 As sediment is a sink for contaminants, its resuspension together with upwelling of TE-enriched  
53 waters have been recognized as important processes responsible for TE recycling in Antarctic  
54 continental shelf (Corami et al., 2005). Seasonal dynamics of sea-ice melting and phytoplankton  
55 production are the main factors controlling the element concentration in seawater: as the sea-ice  
56 formation sequesters dissolved and particulate nutrients and TEs in winter, the following sea-ice  
57 melting, during the austral summer, releases them again in the surface water, fuelling pelagic  
58 production (Frache et al., 2001; Grotti et al., 2005; Illuminati et al., 2017). At the same time, pack-  
59 ice is a seasonal habitat for many microscopic organisms (hereafter called “sympagic organisms”)  
60 which represent additional sources of organic matter and TEs for pelagic consumers as soon as  
61 ice melts, and also for benthic organisms once settled on the seafloor (Grotti et al., 2005; Morata et  
62 al., 2011). High TE levels have been reported also in other terrestrial and marine primary  
63 producers, like moss, lichens (Bargagli et al., 2005) and macroalgae (Runcie and Riddle, 2004), as  
64 well as in many pelagic and benthic consumers at different trophic levels, from zooplankton (Kahle  
65 and Zauke, 2003), to benthic ascidiaceans, anthozoans, sponges, echinoderms, polychaetes and  
66 crustaceans (e.g. Cipro et al., 2017; Grotti et al., 2008; Negri et al., 2006; Trevizani et al., 2016) up  
67 to pelagic and benthic fish (Bustamante et al., 2003). Moreover, most scientific literature regarding  
68 TE accumulation focused on penguins, which have been identified as suitable Hg bioindicators in  
69 the polar areas (Becker et al., 2016; Calle et al., 2015; Carravieri et al., 2013; Nygård et al., 2001).  
70 Despite the great effort made so far, the knowledge of TE transfer processes is still scanty and  
71 represents a critical missing piece in the framework of TE contamination in the Antarctic area. In  
72 particular, despite the acknowledged key ecological and trophic role of phytoplankton and sea ice-  
73 algae in the Southern Ocean (Petrou et al., 2016), as well as their tendency to bioaccumulate a  
74 wide range of TEs, very little is still known about their role as potential element transfer to upper  
75 trophic levels. Moreover, the majority of research on contaminant biomagnification focused on  
76 single elements (e.g. Hg, Bargagli et al., 1998; Cipro et al., 2017) or only a few taxa (Carravieri et  
77 al., 2013; Majer et al., 2014). In turn, the importance of organic matter pathways in the relocation of  
78 TEs along food web is poorly investigated, limiting the ability to predict how variations in sea-ice

79 dynamics and primary production due to climate change will affect TE transfer across species and  
80 trophic levels

81 Owing to the robustness of  $\delta^{13}\text{C}$  in the identification of basal sources of dietary carbon, and the  
82 good correlation between  $\delta^{13}\text{N}$  and trophic level of the organisms in food webs (Post, 2002; Vizzini  
83 et al., 2016), the use of stable isotopes is highly suitable to evaluate the role of horizontal (i.e.  
84 reliance of consumers on different basal sources and trophic pathways) and vertical food web  
85 structure (i.e. trophic positions) in the TE transfer. In particular, as organic matter sources are  
86 typically well distinct based on  $\delta^{13}\text{C}$  signatures (Fry and Sherr, 1989) especially in Antarctica  
87 (Norkko et al., 2007, Calizza et al. 2018), and consumers reflect the  $\delta^{13}\text{C}$  of prey plus only a low  
88 fractionation value (0-1‰) (De Niro and Epstein, 1978), positive or negative relationship between  
89 TEs and  $\delta^{13}\text{C}$  of consumers will reveal the importance of the underlying  $^{13}\text{C}$ -enriched vs.  $^{13}\text{C}$ -  
90 depleted organic matter pathways in TE transfer from basal sources to consumers. In contrast, the  
91 positive or negative relationship between TEs and  $\delta^{15}\text{N}$  of all the organisms belonging to the food  
92 web indicates TE biomagnification or biodilution along food webs (e.g. Nfon et al., 2009; Signa et  
93 al., 2013).

94 In recent years, significant changes in sea ice extent and seasonal dynamics have been observed  
95 at the poles, leading to dramatic ecological consequences in productivity and trophic patterns (Post  
96 et al., 2013; Constable et al. 2014). As the sea ice thickness and seasonal melting are critical to  
97 ensure the subsequent timing of ice algal and phytoplankton blooms and their vertical distribution,  
98 the predicted changes in sea ice cover and thickness and the consequent shift in frequency,  
99 magnitude and availability of sympagic/planktonic production may certainly propagate across  
100 trophic level through bottom-up processes (Constable et al., 2014). Moreover, benthic macroalgae  
101 are known to benefit from higher temperature, light (due to ice thinning) and increased nutrient load  
102 from meltwater, hence higher macroalgae abundance in the shallow area of the Antarctic coasts is  
103 also expected from climate change predictions (Clark et al., 2013), with repercussions on trophic  
104 web structure.

105 As timing and quantity of primary production in Antarctica are expected to change in the future,  
106 with consequence on food web structure and functioning (Constable et al., 2014; Post et al., 2013),

107 understanding the extent of TE transfer is extremely important nowadays. In particular, it is  
108 extremely important to disentangle if and how diet and organic matter pathways (benthic,  
109 planktonic or sympagic) drive the transfer of trace elements to the biota. This will also help to  
110 clarify if species across trophic levels are able to buffer (i.e. biodilute) TE transfer to top predators,  
111 as observed in lower latitude food webs (Signa et al., 2017a). Therefore, the main aim of this paper  
112 was to assess and identify the pathways of trace elements (Cd, Cr, Co, Cu, Hg, Ni, Pb, V) in the  
113 food web of Tethys Bay (Terra Nova Bay, Ross Sea, Antarctica). To do this, the food web structure  
114 was first characterized through stable isotopes ( $\delta^{13}\text{C}$  and  $\delta^{15}\text{N}$ ). After that, the influence of the  
115 horizontal food web structure (i.e. reliance of consumers on different basal sources and trophic  
116 pathways) in TE transfer to consumers was assessed through linear regressions between TEs and  
117  $\delta^{13}\text{C}$ , while the role of the vertical food web structure (i.e. trophic positions) and the occurrence of  
118 biomagnification was evaluated through linear regressions between TEs and  $\delta^{15}\text{N}$  and computation  
119 of the trophic magnification factor (TMF). We hypothesised that i) pelagic primary producers,  
120 namely phytoplankton and sympagic algae, play an important role in the TE transfer to primary  
121 consumers, with potential repercussions in the contamination level of top predators ii) diet and  
122 trophic position are also important drivers for TE transfer to the upper trophic level of the food web  
123 of Tethys Bay, in the Ross Sea.

124

## 125 **2. Materials and methods**

### 126 **2.1 Study area and sampling**

127 Sampling was performed at Tethys Bay, (Terra Nova Bay, Ross Sea, Antarctica) ( $74^{\circ}41'40''\text{S}$   
128  $164^{\circ}03'22''\text{E}$ ), at the end of January 2013 (austral summer). The bay extends 3 km from the inner  
129 to the outer limit and is connected to the open waters of the polynya of Terra Nova Bay. The  
130 seafloor is characterized by rocky and muddy patches, and benthic vegetation coverage is  
131 generally scarce.

132 Evident sea-ice melting and cracking in the bay started ten days before sampling and sea-ice  
133 broke up three days before sampling. Sea-ice coverage and primary productivity in the bay are

134 characterised by marked seasonality, with periods of complete absence of ice coverage and  
135 phytoplankton blooms typically observed in January. Further information on the study area can be  
136 found in Faranda et al., (2000) and Norkko et al., (2007).

137 Methods for basal source and invertebrate collection are reported in Calizza et al. (2018). Briefly,  
138 benthic invertebrates were sampled along linear transects by dredging in medium-depth waters  
139 (40-200m) and by scuba diving in shallow waters (15-25m). Fish were collected through fish lines  
140 and creels which allowed to sample both the benthic habitat and the water column. Bird feathers of  
141 adult Adelie penguins and skua were collected by hand from recently died organisms. Resources  
142 potentially contributing to the diet of secondary consumers were also collected, including (i) benthic  
143 organic matter sources [sediment and coarse (> 2mm) organic detritus] and primary producers (the  
144 red macroalgae *Iridaea cordata* and *Phyllophora antarctica*) were also collected by dredging and  
145 scuba diving in shallow and deep waters; (ii) planktonic primary producers and consumers  
146 (respectively phytoplankton and zooplankton) were collected with a plankton net (20 µm mesh  
147 size) at a depth of 100 m. Zooplankton was carefully separated from the rest of the bulk sample by  
148 hand under a stereoscope. To obtain phytoplankton, the remaining sample was filtered at 100 µm  
149 and collected on pre-combusted Whatmann GF/F filters; (iii) sympagic primary producers  
150 (microscopic and filamentous algae growing both within the ice and at the interface between sea-  
151 ice and water) were collected in November 2012, before sea-ice broke up, by coring the pack-ice  
152 at two sites in the inner and outer part of the bay. Interface algae (i.e. the 2 cm bottom layer of the  
153 core) were considered separately from those growing within the core (i.e. between 2 cm and 1 m  
154 from the bottom, hereafter “core algae”).

155

## 156 **2.2 Laboratory activities**

157 For both isotopic and trace element (TE) analysis, soft tissues of all invertebrate and vertebrate  
158 species/taxa ranging across trophic levels and trophic guilds were considered (Table S1). All  
159 samples were stored at -80 °C at the “Mario Zucchelli” Italian Research Station, and at -20°C  
160 during transportation to Italy, where, after freeze-drying, they were ground using a ball mill (Mini-  
161 Mill Fritsch Pulverisette 23: Fritsch Instruments, Idar-Oberstein, Germany).

162

### 2.2.1 Isotopic analysis

163 When necessary, samples were pre-acidified (HCl 1 M) to eliminate inorganic carbon, which can  
164 interfere with the  $\delta^{13}\text{C}$  signature (Carabel et al., 2006). Un-acidified powder from each sample was  
165 also analysed in order to obtain the  $\delta^{15}\text{N}$  signature, which is known to be affected by HCl exposure  
166 (Carabel et al., 2006). Then, samples underwent stable isotope analysis (SIA) by means of a  
167 continuous flow mass spectrometer (IsoPrime100, Isoprime Ltd., Cheadle Hulme, UK) coupled with  
168 an elemental analyser (Elementar Vario Micro-Cube, Elementar Analysensysteme GmbH,  
169 Germany). Each sample was analysed in two replicates, and isotopic signatures were expressed in  
170  $\delta$  units ( $\delta^{13}\text{C}$ ;  $\delta^{15}\text{N}$ ) as the per mil (‰) difference with respect to standards:  $\delta X (\text{‰}) = [(R_{\text{sample}} -$   
171  $R_{\text{standard}})/R_{\text{standard}}] \times 10^3$ , where X is  $^{13}\text{C}$  or  $^{15}\text{N}$  and R is the corresponding ratio of heavy to light  
172 isotopes ( $^{13}\text{C}/^{12}\text{C}$  or  $^{15}\text{N}/^{14}\text{N}$ ) (Post, 2002). The reference materials used were the international  
173 Vienna PeeDee Belemnite (PDB) as a standard for carbon, and atmospheric nitrogen ( $\text{N}_2$ ) for  
174 nitrogen. Measurement errors were found to be typically smaller than 0.05‰. For  $\delta^{13}\text{C}$ , outputs  
175 were corrected for lipid content (Post et al., 2007) based on the C/N ratio (not reported) of each  
176 sample.

177

### 2.2.2 Trace element analysis

178 For quantification of trace elements (TEs: Cd, Co, Cr, Cu, Hg, Ni, Pb and V), ground samples were  
179 mineralised in an automatic microwave digestion system (MARS 5, CEM): sediment was analysed  
180 using a solution of 67–70%  $\text{HNO}_3$ , 30% HF, 30%  $\text{H}_2\text{O}_2$  and Milli-Q water at a ratio of 6:2:0.4:1.6,  
181 while biological tissues using 67–70%  $\text{HNO}_3$ , 30%  $\text{H}_2\text{O}_2$ , and Milli-Q water at a ratio of 5:1:4. Then,  
182 mineralized samples were analysed by inductively coupled plasma optical emission spectrometry  
183 (ICP-OES, Optima 8000, PerkinElmer). Concentrations of Hg were determined using a hydride  
184 generation system linked to the ICP-OES with a reductant, consisting of 0.2% sodium (Na)  
185 borohydride and 0.05% Na hydroxide.

186 Analytical quality control was performed using Certified Reference Materials (CRMs): Marine  
187 sediment NIST 2702 (National Institute of Standards and Technology) for sediments, *Lagarosiphon*  
188 *major* BCR®–060 (Institute for Reference Materials and Measurements) for primary producers,

189 Fish protein DORM-4 (National Research Council of Canada) for vertebrates and Oyster tissue  
190 1566b NIST® (National Institute of Standards and Technology) for invertebrates. The recovery was  
191 84 to 101%. The detection limit was calculated as three times the standard deviation for digestion  
192 blanks (n > 20) and was similar for all analysed TEs, corresponding to 0.003 mg kg<sup>-1</sup> dw. All results  
193 are given in mg kg<sup>-1</sup> dw.

194

### 195 **2.3 Data elaboration and statistics**

196 The biotic samples analysed were grouped into eight categories (Table S1). In detail, organic  
197 matter sources were grouped in: sediment (SED) including sedimentary organic matter and  
198 detritus; sympagic algae (SYMP) including core and interface sea-ice algae; phytoplankton  
199 (PHYTO-P); phytobenthos (PHYTO-B) including the two rodophyta *I. cordata* and *P. antarctica*.  
200 Consumers were grouped in: zooplankton (ZOO-P) including the *Clione limacina* (Gastropoda),  
201 copepods and euphasiids; zoobenthos (ZOO-B) including the invertebrate benthic species  
202 *Adamussium colbecki* (Bivalvia), *Odontaster validus* (Asteroidea), *Sterechinus neumayeri*  
203 (Echinoidea), *Ophiontus victoriae* (Ophiuroidea) plus unidentified specimens of the genus *Halicona*  
204 (Demospongiae) and others belonging to Cucumaridae (Holoturoidea), Alcyonacea (Anthozoa),  
205 and Polychaeta; fish species (FISH) including *Artedidraco orianae*, *A. skottsbergi*, *Chionodraco*  
206 *hamatus*, *Lepidonotothen nudifrons*, *Trematomus bernacchii*, *T. hansonii*, *T. newnessi* and *T.*  
207 *pennellii*; and birds (BIRDS) including the penguin *Pygoscelis adeliae* and the Antarctic Skua  
208 *Stercorarius antarcticus*. Analyses focused on these targets because they include the most  
209 common species within their respective trophic guilds in the study area, as well as in Antarctic  
210 coastal communities.

211 Differences in the isotopic values among categories were tested by means of a non parametric  
212 MANOVA (NPMANOVA) based on Euclidean distances (Calizza et al., 2017, 2013) followed by  
213 post-hoc tests. The significance is computed by permutation of group membership, with 10000  
214 replicates.



215 Differences in trace elements (TE) concentration between the eight categories were tested through  
216 permutational analysis of variance (PERMANOVA) carried out for each TE based on the Euclidean  
217 distance matrix obtained by normalised TE data, followed by pairwise tests.

218 Identification of principal OM pathways of the food web was carried out using a qualitative  
219 approach. Differences in  $\delta^{13}\text{C}$  values have been shown to provide information on the contribution  
220 of sympagic vs. benthic and pelagic sources to the diet of Antarctic consumers (Calizza et al.,  
221 2018; Norkko et al., 2007), reliably reflecting differences in OM pathways between organisms  
222 (Careddu et al., 2015; Rossi et al., 2015; Signa et al., 2017b). Similarly,  $\delta^{15}\text{N}$  values are known to  
223 increase unequivocally across trophic levels, and therefore, provide a robust base to identify  
224 trophic position of consumers within food webs (Mancinelli et al., 2013; Post, 2002)

225 The effect of the horizontal and vertical food web structure (i.e. organic matter pathways and  
226 trophic position) in shaping the TE pathways within the Antarctic trophic web was assessed  
227 through linear regressions between the logarithm of TEs as the dependent variable and  $\delta^{13}\text{C}$  and  
228  $\delta^{15}\text{N}$  respectively as independent variables. In the first regressions ( $\log[\text{TE}]$  vs.  $\delta^{13}\text{C}$ ), the role of  
229 primary producers and sediment as TE sources was tested separately for primary and secondary  
230 consumers to distinguish potential different patterns. Classification of consumers in primary and  
231 secondary consumers was carried out in advance through identification of suitable  $\delta^{15}\text{N}$  thresholds  
232 coupled with literature comparison of feeding habits: mean  $\delta^{15}\text{N}$  of primary consumers ranged  
233 between  $4.8 \pm 0.8$  and  $6.2 \pm 1.5$  ‰ and  $\delta^{15}\text{N}$  of secondary consumers ranged between  $6.0 \pm 0.5$   
234 and  $9.6 \pm 1.2$  ‰ (Table S1). In contrast, in the second regressions ( $\log[\text{TE}]$  vs.  $\delta^{15}\text{N}$ ), all the biotic  
235 samples were included to assess the biomagnification/biodilution patterns along the whole food  
236 web. Residual analysis was performed in both cases to ensure that assumptions were not violated.  
237 If outliers were identified, they were removed and the regression analysis was performed again.  
238 Trophic magnification factors (TMF) was also calculated based on  $\log[\text{TE}]$  vs.  $\delta^{15}\text{N}$  linear  
239 regressions to quantify the biomagnification ( $\text{TMF} > 1$ ) or biodilution ( $\text{TMF} < 1$ ) power of the trace  
240 elements studied along the food web. TMF was computed as follows, according to Borgå et al.  
241 (2011):  $\text{Log}[\text{TE}] = a + b(\delta^{15}\text{N})$ ;  $\text{TMF} = 10^b$ .

242

## 243 **3. Results**

### 244 **3.1 Isotopic signatures**

245 Isotopic distribution differed between all groups analysed (NPMANOVA  $F = 30.2$ ,  $p < 0.0001$ , and  
246 associated post-hoc tests,  $p$  always  $< 0.05$ ) (Table S2), with the exception of fish and birds, which  
247 do not differed significantly ( $p > 0.05$ ). Specifically, isotopic distributions of the four main basal  
248 resource guilds (i.e. phytoplankton, phytobenthos, sedimentary organic matter and sympagic  
249 algae) differed either for their  $\delta^{13}\text{C}$  and/or the  $\delta^{15}\text{N}$  values (Fig. 1). Basal resources occupied a  
250  $\delta^{13}\text{C}$  range much wider than that occupied by invertebrates and vertebrate consumers which, in  
251 turn, mainly differed for their  $\delta^{15}\text{N}$  values.

252

### 253 **3.2 Trace elements**

254 Trace element (TE) analysis revealed different patterns both among sample categories and TEs  
255 (Fig. 2). Cr, Pb, Ni and V showed similar trends, with overall significantly higher concentrations in  
256 organic matter sources than in consumers. In particular, Cr peaked in phytoplankton, followed by  
257 sediment and sympagic algae, while benthic macroalgae (PHYTO-B) reported similar  
258 concentrations to zooplankton and birds. In contrast, Ni, Pb and V showed the highest  
259 concentration in both phytoplankton and sediment, followed by sympagic and benthic macroalgae,  
260 which showed values overall comparable to birds and zooplankton (Ni, Pb) and zoobenthos (V).  
261 Cu concentration in phytoplankton was also high, but the highest values were recorded in  
262 sympagic algae. The other source and consumer categories highlighted similar lower values with  
263 the lowest ones recorded in fish. Co concentration peaked in sediment, followed by all the other  
264 categories with evenly lower values. In contrast, Hg levels were significantly higher in birds than in  
265 all the other categories, among which fish showed the highest concentration, followed by benthic  
266 invertebrates, sympagic algae and phytoplankton as an homogeneous group, and the others with  
267 the lowest values. Finally, Cd did not show a clear trend and the highest values were observed in  
268 benthic invertebrates, phytoplankton and phytobenthos, followed by zooplankton and sympagic  
269 algae.

270 In primary consumers, only Hg, Pb and V were significantly correlated with  $\delta^{13}\text{C}$ , with the first two  
271 elements negatively, and only the latter positively correlated, while in secondary consumers, the  
272 correlation was significant and positive for Cd and Hg, and negative for Ni and Pb (Fig. 3 and  
273 Tab.1). Pb decreased along  $\delta^{13}\text{C}$  in both primary and secondary consumers, while Cd and Hg had  
274 an opposite trend in the two groups, decreasing in primary consumers and increasing in secondary  
275 consumers (Fig. 3).

276 Linear regressions between  $\log[\text{TE}]$  and  $\delta^{15}\text{N}$  of the whole food web components, organic matter  
277 sources and consumers, highlighted a similar behaviour of all TEs, except for  $\log[\text{Hg}]$  (Fig. 4 and  
278 Tab.1). Indeed, the log values of the concentration of TEs decreased as the  $\delta^{15}\text{N}$  increased,  
279 indicating TE biodilution along the food web, while only  $\log[\text{Hg}]$  increased along  $\delta^{15}\text{N}$  values,  
280 suggesting Hg biomagnification across trophic levels (Fig. 4). These patterns were confirmed by  
281 the trophic magnification factor (TMF), which was lower than 1 for all TEs except for Hg whose  
282 TMF was 1.23 (Fig. 4). Both negative and positive correlations were all highly significant (Table 1).

283

## 284 **4. Discussion**

### 285 **4.1 Food web structure**

286 Isotopic values of the organic matter sources from Tethys Bay, Ross Sea (Antarctica) covered a  
287 wide  $\delta^{13}\text{C}$  range ( $\Delta^{13}\text{C}= 31.2\text{‰}$ ) varying from the highly depleted values of the benthic red  
288 macroalga *Phyllophora antarctica*, to the highly enriched ones of sympagic algae. The other red  
289 macroalga *Iridaea cordata*, phytoplankton and sediment organic matter showed intermediate and  
290 overlapped values. The large differences in  $\delta^{13}\text{C}$  signatures among primary producers is not new in  
291 the Antarctic region and current results are consistent with previous studies (Gillies et al., 2012;  
292 Norkko et al., 2007, Calizza et al. 2018). In particular, the high variability found within the sympagic  
293 algae group is due to the different  $\delta^{13}\text{C}$  signature of interface and core ice-algae, probably  
294 associated to diverse taxonomic composition (mainly diatoms vs. filamentous algae respectively).  
295 In addition, high seasonality in the isotopic values of the particulate organic matter (POM) is typical  
296 of the Antarctic region because of the different environmental conditions, and especially the strong

297 seasonality of ice coverage and primary production (Cozzi and Cantoni, 2011). Accordingly, the  
298 more depleted values of the core algae may be linked to the highly negative  $\delta^{13}\text{C}$  signature of POM  
299 in the winter period (-30 to -21%, Kennedy et al., 2002) during sea-ice formation. In contrast, the  
300 more enriched values of the interface algae may also reflect the isotopic enrichments occurring  
301 during the spring ice-algae bloom and then with the presence of freshly produced algal biomass  
302 (Cozzi and Cantoni, 2011; Norkko et al., 2007). The horizontal food web structure of Tethys Bay  
303 was characterised by two main trophic pathways, the first based on phytoplankton, sediment and  
304 the benthic macroalga *I. cordata*, and the second one based on sympagic algae. The highly  $^{13}\text{C}$ -  
305 depleted values of the other macroalga, *P. antarctica*, was out from the isotopic space  
306 encompassing the other primary producers and the consumers. Consequently, we may infer that  
307 *P. antarctica* does not enter in the Tethys Bay food web, unless in a detrital form, because of the  
308 abundance of polyphenols that protect it from grazers (Norkko et al., 2007; Calizza et al. 2018).  
309 Unlike organic matter sources, consumers grouped mostly based on their  $\delta^{15}\text{N}$  signatures and  
310 showed a rather narrow  $\delta^{13}\text{C}$  range, except for zoobenthos, which spanned a wide range as effect  
311 of a variable contribution of benthic/planktonic sources and sympagic algae in their diet (Calizza et  
312 al., 2018). Despite narrower, the  $\delta^{15}\text{N}$  range of the zoobenthos suggests that benthic invertebrates  
313 belong to two trophic levels, including both primary and secondary consumers. Indeed, Antarctic  
314 benthic invertebrates vary greatly in the feeding habits, from grazers, filter feeders and  
315 depositivores to predators and scavengers (Corbisier et al., 2004), and exhibit also a high degree  
316 of trophic plasticity and omnivory (Norkko et al., 2007). In contrast, the narrow  $\delta^{13}\text{C}$  range coupled  
317 with the wide  $\delta^{15}\text{N}$  range reveal that zooplankton relies mostly on other planktivorous species  
318 although a certain influence of phytoplankton and core sympagic algae in the diet cannot be ruled  
319 out, therefore showing an omnivorous feeding strategy (Tamelander et al., 2008). Lastly, the  
320 highest  $\delta^{15}\text{N}$  signatures of fish and birds and their intermediate position within the  $\delta^{13}\text{C}$  range,  
321 highlight the role as top predators that couple the underlying resource pathways, as previously  
322 documented in Arctic (McMeans et al., 2013) and temperate marine systems (Vizzini et al., 2016).

323

## 324 **4.2 Trace element levels in food web components**

325 Sediment trace element (TE) concentration measured in this study was overall comparable to  
326 previous studies carried out in the Ross Sea (Grotti et al., 2008; Ianni et al., 2010) with the  
327 exception of Pb and Hg, which showed higher values compared with existing literature (Pb: Grotti  
328 et al., 2008; Ianni et al., 2010; Hg: Bargagli et al., 1998; Negri et al., 2006). The elevated pelagic  
329 primary productivity of the Antarctic system (Petrou et al., 2016), together with the high TE levels in  
330 the dissolved compartment (Corami et al., 2005; Sañudo-Wilhelmy et al., 2002), highlight the  
331 important role of this component within the food web and also its enrichment in TEs, thus  
332 representing a potential source of TEs for both pelagic and benthic consumers (once settled on the  
333 seafloor) (Cabrita et al., 2017; Deheyn et al., 2005). Similarly, sympagic algae are known to be a  
334 good bioaccumulator of nutrients and TEs, which are entrapped within the pack-ice during winter,  
335 becoming then bioavailable in summer, as soon as the pack-ice starts to melt (Grotti et al., 2005,  
336 Pusceddu et al. 2009, Calizza et al. 2018). Present results confirm previously recorded high TE  
337 levels, as phytoplankton and core sympagic algae (sampled in spring before the beginning of the  
338 ice melting) showed overall the highest TE concentration among primary producers, giving an  
339 indication of their potential in the TE transfer pathway to both pelagic and benthic consumers. In  
340 more detail, phytoplankton reached TEs levels from 2-fold (Hg) to 4- (Cd) and even 10-fold (Pb)  
341 higher than those previously recorded in the same area (Bargagli et al., 1998, 1996; Cabrita et al.,  
342 2017; Dalla Riva et al., 2003).

343 As regards consumers, only Cd, Cu and Hg revealed remarkable TE concentration. High Cd levels  
344 in both primary producers and consumers (except for vertebrates) were already observed in Terra  
345 Nova Bay by Bargagli et al. (1996) who defined it as “the Cd anomaly”. The authors explained this  
346 phenomenon as the effect of the upwelling of Cd-enriched deep waters, which makes this element  
347 available to primary producers and then to primary consumers through trophic transfer. Copper  
348 showed accumulation patterns similar to Cd, consistently with the findings by Grotti et al. (2008),  
349 while Hg concentration and pattern suggest biomagnification, as previously documented in the  
350 same area (Bargagli et al., 1998) and other polar and temperate areas (e.g. Nfon et al., 2009;  
351 Signa et al., 2017), with the highest concentration in top predators and the lowest ones at the base  
352 of the food web. The highest Hg levels were found in bird feathers, especially in those of the brown

353 skua (*Stercorarius antarcticus*) consistent with the values observed in various skua populations  
354 from many Antarctic areas (Becker et al., 2016).

355

### 356 **4.3 Horizontal and vertical food web structure drives trace element transfer**

357 Isotopic results from this study indicated that two pathways, sympagic and benthic/planktonic  
358 (indistinguishable based on the samples analysed here) flow through the food web of Tethys Bay  
359 and are coupled by top predators, similar to the food web studied by McMeans et al. (2013) in the  
360 Arctic system. The clear  $\delta^{13}\text{C}$  trend of the organic matter sources, varying from the highly depleted  
361 red macroalga *P. antarctica* to a homogenous more  $^{13}\text{C}$ -enriched group made of the red macroalga  
362 *I. cordata*, sediment and phytoplankton, up to the most  $^{13}\text{C}$ -enriched sympagic algae, allowed the  
363 identification of relevant patterns in TE transfer. Indeed, linear regressions between consumer  
364  $\log[\text{TE}]$  and  $\delta^{13}\text{C}$  highlighted that the trophic pathway based on sympagic algae was not relevant in  
365 driving TE transfer to primary consumers, unless for V. In contrast, the significant and positive  
366 correlation between both  $\log[\text{Cd}]$  and  $\log[\text{Hg}]$  vs.  $\delta^{13}\text{C}$  revealed the importance of the sympagic  
367 pathway in the transfer of these two elements up to secondary consumers. This not consistent Cd  
368 and Hg pattern between primary and secondary consumers may depend on the low number of  
369 primary consumers relying on sympagic algae sampled in this study. Indeed, among all, only some  
370 specimens of Alcyonacea, filter feeder polychaetes and the sea urchin *Sterechinus neumayeri*  
371 showed the reliance on sympagic algae as a food source, while also other benthic species, such  
372 as the detritivores and suspension feeders *Flabelligera mundata*, *Laternula elliptica*, *Paramoera*  
373 *walkeri* rely on this resource in the Antarctic region (Wing et al., 2012). This is due to vertical pulse  
374 of ice algae-derived organic matter to the deep layers of polar areas that is an important process  
375 which contribute to a tight pelagic-benthic coupling (Morata et al., 2011). Looking at secondary  
376 consumers, only the sea star *Odontaster validus* showed high Cd and Hg levels derived from the  
377 sympagic trophic pathway. Being a benthic active predator, feeding mainly on invertebrates (Dalla  
378 Riva et al., 2004) but including also other items in the diet, due to a marked omnivorous feeding  
379 behaviour (Norkko et al., 2007), the direct reliance on sympagic algae, when available, cannot be  
380 ruled out.

381 Primary consumers, for which incorporation of sediment and phytoplankton advected from the  
382 upper water column layers was more likely, showed generally higher but also more variable Cd  
383 and Hg accumulation. In particular, as mainly filter feeders (filter feeder holothuroidea, polychaeta  
384 and sponges) grouped in the upper left side of the graphs due to the high Cd and Hg  
385 concentration, we may infer that phytoplankton is the main driver of Cd and Hg in the benthic  
386 habitat of Tethys Bay. Moreover, phytoplankton in the study are has been shown to present lower  
387  $\delta^{13}\text{C}$  (Calizza et al., 2018) than those found here, further strengthening this hypothesis.

388 Lead was the only element with an opposite trend, significantly decreasing as the  $\delta^{13}\text{C}$  increased in  
389 both primary and secondary consumers, suggesting that settled phytoplankton, macroalgae and  
390 sediment represent also important Pb sources for invertebrates in Tethys Bay. Lead is defined as a  
391 “scavenging type” element that typically shows increasing concentration at higher depths (Frache  
392 et al., 2001; Illuminati et al., 2017), hence this behaviour may have contributed to the observed  
393 patterns. Indeed, Illuminati et al., (2017) found that the effect of the sea ice melting on Pb seawater  
394 content is not relevant in summer, being the surface water layer (~15 m depth) mostly interested  
395 by atmospheric deposition and wet deposition from continental land (Dalla Riva et al., 2003), while  
396 the sinking of biogenic particles following the phytoplankton bloom affects the Pb level in the  
397 deeper layers (~100m - same maximum depth where the phytoplankton was sampled in this  
398 study). Our isotopic results, in agreement with literature findings (Elias-Piera et al., 2013; Norkko et  
399 al., 2007), support the hypothesis that benthic macroalgae, sediment and phytodetritus are  
400 important organic matter sources in the trophic web of Tethys Bay, hence representing relevant  
401 sources of Pb for many organisms with potential detrimental effects.

402 As regards the other TEs for which any significant pattern was identified, especially Co, Cr and Cu,  
403 it could be argued that a conjoint contribution of all sources in the TE transfer to consumers takes  
404 place, rather than having no role in TE transfer. Indeed, as previously mentioned, omnivory and  
405 trophic plasticity are widely diffused in the polar food webs, mainly due to the high influence of  
406 seasonality in primary production that requires continuous adaptation in the selection of food by the  
407 fauna (Norkko et al., 2007; Tamelander et al., 2008) and may have contributed to the observed  
408 patterns. Moreover, it should be noticed that TE bioavailability and transfer to the biota are highly

409 element- and species-specific resulting from many factors, from sediment physicochemical  
410 properties, to the specie-specific routes of exposure and detoxification processes (Signa et al.,  
411 2017a). Although the study of such processes was not in the scope of this research, their  
412 occurrence cannot be ruled out when the patterns between TEs and carbon isotopic signature  
413 were not clear.

414 Linear regression between trace elements and  $\delta^{15}\text{N}$ , used as a proxy for trophic position (Post,  
415 2002), were highly significant for all the elements analysed. However, only total mercury (Hg)  
416 biomagnified along the food web of Tethys Bay, as indicated by the positive slope together with the  
417 trophic magnification factor (TMF)  $> 1$ , which is a proxy for the biomagnification power. In  
418 particular, the values of the slope (0.09) and TMF (1.23) were consistent with the lower values of  
419 the range published, due to the use of total Hg, instead of Me-Hg, together with the large variety of  
420 trophic levels within the food web studied (Signa et al., 2017c), while most biomagnification studies  
421 often focuses on only partial food webs and trophic levels. Indeed, the pivotal study of Bargagli et  
422 al. (1998) was the first and the only one describing such Hg behaviour in Terra Nova Bay, by  
423 comparing Hg concentration in many organisms belonging to different trophic levels, from  
424 phytoplankton to penguins. After that, subsequent studies confirmed this trend (Cipro et al., 2017),  
425 although some of them focused on only a part of the food web, namely benthic organisms (Majer et  
426 al., 2014) and penguins (Calle et al., 2015; Carravieri et al., 2013; Nygård et al., 2001). Present  
427 results confirm that trophic position plays the key role in the Hg levels and relocation in the food  
428 web of Tethys Bay, although other factors also contribute in determining the differing Hg  
429 concentration observed in organisms with similar trophic position. Indeed, benthic fauna showed  
430 higher Hg concentrations than zooplankton, although their overlapped isotopic signatures, and it  
431 may be explained by the higher Hg exposure in the benthic vs. pelagic compartment, as Hg  
432 methylation and photodemethylation occur respectively in sediments and seawater resulting  
433 respectively in an increase and decrease of Hg bioavailability (Goutte et al., 2015). Similarly,  
434 seabirds and fish showed an overlapped isotopic niche but different Hg concentration, probably  
435 mirroring different diet or foraging habitat. In particular, Adélie penguins, which feed preferentially  
436 on ice-krill and pelagic fish (Ainley, 2002), share  $\delta^{15}\text{N}$  and Hg ranges with benthic predatory fish



437 (i.e. *Artedidraco orianae*, *A. skottsbergi* and *Trematomus hansonii*), whose main prey are benthic  
438 invertebrates belonging to various trophic levels (La Mesa et al., 2004). Hence, the effect of a  
439 different diet seems to counterbalance the effect of the different feeding habitat resulting in an  
440 overlapped  $\delta^{15}\text{N}$  and Hg signature. In contrast, the brown skua *S. antarcticus* is known as predator  
441 and scavenger feeding on bird carrions (Becker et al., 2016). This diet is consistent with the role of  
442 top predator, justifying the high Hg level found, but is not consistent with the concurrent low  $\delta^{15}\text{N}$   
443 values in feathers, which are probably the result of the reliance of a wide range of prey in the  
444 previous inter-breeding season spent in the Sub-Antarctic and Subtropical zones (Cherel et al.,  
445 2017).

446 Unlike Hg, all the other TEs (i.e. Cd, Cr, Co, Cu, Ni, Pb, V) showed significant opposite patterns  
447 that, concurrent with  $\text{TMF} < 1$ , indicated a biodiluting behaviour along the food web. This is  
448 consistent with previous studies carried out both in polar (Nfon et al., 2009) and temperate areas  
449 (Signa et al., 2017c), which showed also similar TMF values, suggesting a univocal pattern,  
450 regardless of geographical area or seasonality. Indeed, biomagnification of other trace elements  
451 besides Hg has been reported infrequently and this common biodilution trend has been attributed  
452 to the efficient TE sequestration and/or excretion abilities of the organisms during the trophic  
453 transfer, concurrent with the growth dilution in the large-bodied species at high trophic levels.

454 Cd deserves a mention apart because of the well-known “Cd anomaly” in the Antarctic area  
455 (Bargagli et al., 1996), which leads to very high Cd concentrations, compared to other marine  
456 systems (Bargagli et al., 1996; Sañudo-Wilhelmy et al., 2002). Moreover, Cd is prone to  
457 bioaccumulate in benthic invertebrates and may biomagnify depending on the organisms involved  
458 (Majer et al., 2014; Signa et al., 2017c). Accordingly, Cd concentration in benthic invertebrates  
459 from Tethys Bay resulted markedly high, contrasting with the very low Cd concentration found in  
460 fish muscle and bird feathers. At a first glance, this result may be interpreted as a biodilution along  
461 trophic levels, but the occurrence of Cd sequestration processes in other tissues may have led to  
462 this result. Indeed, although the muscle tissue represents the stable pool of trace elements for fish  
463 (Barwick and Maher, 2003), Cd is more efficiently sequestered by fish in liver and kidney, than in  
464 muscle (Bargagli et al., 1996; Bustamante et al., 2003) . Therefore, while muscle is considered the

465 most appropriate tissue for isotopic description of feeding habit and trophic position in fish  
466 (Costantini et al. 2018), the low Cd concentration found here does not mean necessarily biodilution  
467 or lack of Cd exposure at the whole organism level, and multi-tissue analysis is needed to clarify  
468 this point.

469

## 470 **5. Conclusions and future perspectives**

471 Trace element (TE) contamination and transfer is a topic of paramount concern worldwide  
472 including the remote Antarctic region, because of the occurrence of natural and anthropogenic  
473 transport processes on local-to-global scales. Despite levels of many trace elements (TE) have  
474 been widely described in single components of the Antarctic food web, the pathways fueling TE  
475 transfer to the biota, taking into account all the food web components, are poorly characterized.  
476 Here, in this first effort to describe the Cd, Cr, Co, Cu, Hg, Ni, Pb and V transfer pathways in Terra  
477 Nova Bay, we provide evidence of the importance of both sympagic and phytoplanktonic pathways,  
478 and trophic position, in driving the TE transfer to the biota. In particular, linear regression analysis  
479 between the log-transformed concentration of TEs and  $\delta^{13}\text{C}$  revealed a significant influence of the  
480 sympagic algae pathway on the Cd and Hg levels of secondary consumers. Phytoplanktonic  
481 pathway was more relevant in the Cd and Hg transfer to primary consumers and in the Pb transfer  
482 to both trophic levels. This is probably because of its higher concentration in the deeper layer due  
483 to the typical Pb “scavenging” behavior. A concurrent role of both patterns was highlighted,  
484 instead, for the other TEs.

485 Despite it turned out that both trophic pathways are coupled by top predators (fish and birds), Hg  
486 was the only chemical whose concentration increased from basal sources to top predators and that  
487 also biomagnified along the food web, as revealed by the significant positive correlation between  
488  $\log[\text{Hg}]$  and  $\delta^{15}\text{N}$  and the trophic magnification factor  $\text{TMF} > 1$ . In agreement with most literature,  
489 the behavior of all the other TEs was opposite to that of Hg, giving evidence of a biodilution along  
490 trophic levels. Nevertheless, the ability of top predators in sequester dietary elements in other  
491 tissues than muscle, leaves an open window to further investigations in the area.

492 Concluding, climate change scenarios forecast a dramatic change in sea-ice extent and dynamics  
493 in polar areas (Constable et al., 2014; Post et al., 2013). In turn, this will produce important  
494 changes in frequency and magnitude of sympagic/planktonic production, with potential shifts in  
495 their relative contribution to the benthic communities (Clark et al., 2013; Constable et al., 2014). In  
496 this context, these data represent a useful reference of present baseline conditions in Terra Nova  
497 Bay (Ross Sea), and revealed that change of trophic pathways could also lead to change of TE  
498 transfer through the Antarctic food web. Indeed, in light of the marked efficiency of benthic  
499 macrofauna in the exploitation of pulsed food sources according to their availability (Calizza et al.,  
500 2018; Mäkelä et al., 2017; Norkko et al., 2007), our findings suggest that changes in food inputs  
501 fuelling the food web may rebound in unprecedented exposure of Antarctic species to TEs, in  
502 terms of a different TE species and concentration, than what experienced in the past.

503

## 504 **6. Acknowledgements**

505 This research was supported by PNRA, projects: PNRA-2013/AZ1.01-L. Rossi, PNRA-  
506 2015/AZ1.01-M.L. Costantini, and PNRA16\_00291-L. Rossi.

507

## 508 **References**

509 Ainley, D.G., 2002. The Adélie penguin: bellwether of climate change. Columbia University Press,  
510 New York, USA.

511 Bargagli, R., 2008. Environmental contamination in Antarctic ecosystems. *Sci. Total Environ.* 400,  
512 212–26. doi:10.1016/j.scitotenv.2008.06.062

513 Bargagli, R., Agnorelli, C., Borghini, F., Monaci, F., 2005. Enhanced deposition and  
514 bioaccumulation of mercury in Antarctic terrestrial ecosystems facing a coastal polynya.  
515 *Environ. Sci. Technol.* 39, 8150–5.

516 Bargagli, R., Monaci, F., Sanchez-Hernandez, J.C., Cateni, D., 1998. Biomagnification of mercury  
517 in an Antarctic marine coastal food web. *Mar. Ecol. Prog. Ser.* 169, 65–76.  
518 doi:10.3354/meps169065

- 519 Bargagli, R., Nelli, L., Ancora, S., Focardi, S., 1996. Elevated cadmium accumulation in marine  
520 organisms from Terra Nova Bay (Antartica). *Polar Biol.* 16, 513–520.  
521 doi:10.1007/BF02329071
- 522 Barwick, M., Maher, W., 2003. Biotransference and biomagnification of selenium copper, cadmium,  
523 zinc, arsenic and lead in a temperate seagrass ecosystem from Lake Macquarie Estuary,  
524 NSW, Australia. *Mar. Environ. Res.* 56, 471–502. doi:10.1016/s0141-1136(03)00028-x
- 525 Becker, P.H., Goutner, V., Ryan, P.G., Gonz, J., González-Solís, J., 2016. Feather mercury  
526 concentrations in Southern Ocean seabirds: Variation by species, site and time. *Environ.*  
527 *Pollut.* 216, 253–263. doi:10.1016/j.envpol.2016.05.061
- 528 Borgå, K., Kidd, K.A., Muir, D.C.G., Berglund, O., Conder, J.M., Gobas, F.A.P.C., Kucklick, J.,  
529 Malm, O., Powell, D.E., 2011. Trophic magnification factors: Considerations of ecology,  
530 ecosystems, and study design. *Integr. Environ. Assess. Manag.* 8, 64–84.  
531 doi:10.1002/ieam.244
- 532 Bustamante, P., Bocher, P., Chérel, Y., Miramand, P., Caurant, F., 2003. Distribution of trace  
533 elements in the tissues of benthic and pelagic fish from the Kerguelen Islands. *Sci. Total*  
534 *Environ.* 313, 25–39. doi:10.1016/S0048-9697(03)00265-1
- 535 Cabrita, M.T., Padeiro, A., Amaro, E., dos Santos, M.C., Leppe, M., Verkulich, S., Hughes, K.A.,  
536 Peter, H.U., Canário, J., 2017. Evaluating trace element bioavailability and potential transfer  
537 into marine food chains using immobilised diatom model species *Phaeodactylum tricornutum*,  
538 on King George Island, Antarctica. *Mar. Pollut. Bull.* 121, 192–200.  
539 doi:10.1016/j.marpolbul.2017.05.059
- 540 Calizza, E., Careddu, G., Sporta Caputi, S., Rossi, L., Costantini, M.L., 2018. Time- and depth-  
541 wise trophic niche shifts in Antarctic benthos. *PLoS One* 13, 1–17.  
542 doi:10.1371/journal.pone.0194796
- 543 Calizza, E., Costantini, M.L., Careddu, G., Rossi, L., 2017. Effect of habitat degradation on

544 competition, carrying capacity, and species assemblage stability. *Ecol. Evol.* 7, 5784–5796.  
545 doi:10.1002/ece3.2977

546 Calizza, E., Costantini, M.L., Carlino, P., Bentivoglio, F., Orlandi, L., Rossi, L., 2013. *Posidonia*  
547 *oceanica* habitat loss and changes in litter-associated biodiversity organization: A stable  
548 isotope-based preliminary study. *Estuar. Coast. Shelf Sci.* 135, 137–145.  
549 doi:10.1016/j.ecss.2013.07.019

550 Calle, P., Alvarado, O., Monserrate, L., Cevallos, J.M., Calle, N., Alava, J.J., Manuel, J., Calle, N.,  
551 José, J., 2015. Mercury accumulation in sediments and seabird feathers from the Antarctic  
552 Peninsula. *Mar. Pollut. Bull.* 91, 410–417. doi:10.1016/j.marpolbul.2014.10.009

553 Carabel, S., Godínez-Domínguez, E., Verísimo, P., Fernández, L., Freire, J., 2006. An assessment  
554 of sample processing methods for stable isotope analyses of marine food webs. *J. Exp. Mar.*  
555 *Bio. Ecol.* 336, 254–261. doi:10.1016/j.jembe.2006.06.001

556 Careddu, G., Costantini, M.L., Calizza, E., Carlino, P., Bentivoglio, F., Orlandi, L., Rossi, L., 2015.  
557 Effects of terrestrial input on macrobenthic food webs of coastal sea are detected by stable  
558 isotope analysis in Gaeta Gulf. *Estuar. Coast. Shelf Sci.* 154, 158–168.

559 Carravieri, A., Bustamante, P., Churlaud, C., Cherel, Y., 2013. Penguins as bioindicators of  
560 mercury contamination in the Southern Ocean: birds from the Kerguelen Islands as a case  
561 study. *Sci. Total Environ.* 454–455, 141–8. doi:10.1016/j.scitotenv.2013.02.060

562 Cherel, Y., Graña Grilli, M., Cherel, Y., 2017. Skuas (*Stercorarius* spp.) moult body feathers during  
563 both the breeding and inter-breeding periods: implications for stable isotope investigations in  
564 seabirds. *Ibis (Lond. 1859)*. 159, 266–271. doi:10.1111/ibi.12441

565 Cipro, C.V.Z., Montone, R.C., Bustamante, P., 2017. Mercury in the ecosystem of Admiralty Bay ,  
566 King George Island , Antarctica : Occurrence and trophic distribution. *Mar. Pollut. Bull.* 114,  
567 564–570. doi:10.1016/j.marpolbul.2016.09.024

568 Clark, G.F., Stark, J.S., Johnston, E.L., Runcie, J.W., Goldsworthy, P.M., Raymond, B., Riddle,

569 M.J., 2013. Light-driven tipping points in polar ecosystems. *Glob. Chang. Biol.* 19, 3749–  
570 3761. doi:10.1111/gcb.12337

571 Constable, A.J., Melbourne-Thomas, J., Corney, S.P., Arrigo, K.R., Barbraud, C., Barnes, D.K.A.,  
572 Bindoff, N.L., Boyd, P.W., Brandt, A., Costa, D.P., Davidson, A.T., Ducklow, H.W., Emmerson,  
573 L., Fukuchi, M., Gutt, J., Hindell, M.A., Hofmann, E.E., Hosie, G.W., Iida, T., Jacob, S.,  
574 Johnston, N.M., Kawaguchi, S., Kokubun, N., Koubbi, P., Lea, M.A., Makhado, A., Massom,  
575 R.A., Meiners, K., Meredith, M.P., Murphy, E.J., Nicol, S., Reid, K., Richerson, K., Riddle,  
576 M.J., Rintoul, S.R., Smith, W.O., Southwell, C., Stark, J.S., Sumner, M., Swadling, K.M.,  
577 Takahashi, K.T., Trathan, P.N., Welsford, D.C., Weimerskirch, H., Westwood, K.J., Wienecke,  
578 B.C., Wolf-Gladrow, D., Wright, S.W., Xavier, J.C., Ziegler, P., 2014. Climate change and  
579 Southern Ocean ecosystems I: How changes in physical habitats directly affect marine biota.  
580 *Glob. Chang. Biol.* 20, 3004–3025. doi:10.1111/gcb.12623

581 Corami, F., Capodaglio, G., Turetta, C., Soggia, F., Magi, E., Grotti, M., 2005. Summer distribution  
582 of trace metals in the western sector of the Ross Sea, Antarctica. *J. Environ. Monit.* 7, 1256–  
583 64. doi:10.1039/b507323p

584 Corbisier, T.N., Petti, M.A.V., Skowronski, R.S.P., Brito, T.A.S., 2004. Trophic relationships in the  
585 nearshore zone of Martel Inlet (King George Island, Antarctica):  $\delta^{13}\text{C}$  stable-isotope analysis.  
586 *Polar Biol.* 27, 75–82. doi:10.1007/s00300-003-0567-z

587 Cozzi, S., Cantoni, C., 2011. Stable isotope ( $\delta^{13}\text{C}$  and  $\delta^{15}\text{N}$ ) composition of particulate organic  
588 matter, nutrients and dissolved organic matter during spring ice retreat at Terra Nova Bay.  
589 *Antarct. Sci.* 23, 43–56. doi:10.1017/S0954102010000611

590 Dalla Riva, S., Abemoschi, M.L., Chiantore, M., Grotti, M., Magi, E., Soggia, F., 2003.  
591 Biogeochemical cycling of Pb in the coastal marine environment at Terra Nova Bay, Ross  
592 Sea. *Antarct. Sci.* 15, 425–432. doi:10.1017/S0954102003001524

593 Dalla Riva, S., Abemoschi, M.L., Magi, E., Soggia, F., 2004. The utilization of the Antarctic  
594 environmental specimen bank (BCAA) in monitoring Cd and Hg in an Antarctic coastal area in

595 Terra Nova Bay (Ross Sea - Northern Victoria Land). *Chemosphere* 56, 59–69.  
596 doi:10.1016/j.chemosphere.2003.12.026

597 De Niro, M.J., Epstein, S., 1978. Influence of diet on the distribution of carbon isotopes in animals.  
598 *Geochim. Cosmochim. Acta* 42, 495–506. doi:10.1016/0016-7037(78)90199-0

599 Deheyn, D.D., Gendreau, P., Baldwin, R.J., Latz, M.I., 2005. Evidence for enhanced bioavailability  
600 of trace elements in the marine ecosystem of Deception Island, a volcano in Antarctica. *Mar.*  
601 *Environ. Res.* 60, 1–33. doi:10.1016/j.marenvres.2004.08.001

602 Elias-Piera, F., Rossi, S., Gili, J.M., Orejas, C., 2013. Trophic ecology of seven Antarctic gorgonian  
603 species. *Mar. Ecol. Prog. Ser.* 477, 93–106. doi:10.3354/meps10152

604 Faranda, F.M., Guglielmo, L., Ianora, A., 2000. The Italian Oceanographic Cruises in the Ross Sea  
605 (1987–95): Strategy, General Considerations and Description of the Sampling Sites, in: *Ross*  
606 *Sea Ecology*. Springer Berlin Heidelberg, pp. 1–13.

607 Frache, R., Abelloschi, M.L., Grotti, M., Ianni, C., Magi, E., Soggia, F., Capodaglio, G., Turetta,  
608 C., Barbante, C., 2001. Effects of ice melting on Cu, Cd and Pb profiles in Ross sea waters  
609 (Antarctica). *Int. J. Environ. Anal. Chem.* 79, 301–313. doi:10.1080/03067310108044391

610 Fry, B., Sherr, E.B., 1989.  $\delta^{13}\text{C}$  measurements as indicators of carbon flow in marine and  
611 freshwater ecosystems, in: Rundel, P.W., Ehleringer, J.R., Nagy, K.A. (Eds.), *Stable Isotopes*  
612 *in Ecological Research*. Springer-Verlag, New York, pp. 196–229.

613 Gillies, C.L., Stark, J.S., Smith, S.D.A.A., 2012. Research article: Small-scale spatial variation of  
614  $\delta^{13}\text{C}$  and  $\delta^{15}\text{N}$  isotopes in Antarctic carbon sources and consumers. *Polar Biol.* 35, 813–  
615 827. doi:10.1007/s00300-011-1126-7

616 Goutte, A., Cherel, Y., Churlaud, C., Ponthus, J.P., Massé, G., Bustamante, P., 2015. Trace  
617 elements in Antarctic fish species and the influence of foraging habitats and dietary habits on  
618 mercury levels. *Sci. Total Environ.* 538, 743–749. doi:10.1016/j.scitotenv.2015.08.103

619 Grotti, M., Soggia, F., Ianni, C., Frache, R., 2005. Trace metals distributions in coastal sea ice of

620 Terra Nova Bay, Ross Sea, Antarctica. *Antarct. Sci.* 17, 289–300.  
621 doi:10.1017/S0954102005002695

622 Grotti, M., Soggia, F., Lagomarsino, C., Dalla Riva, S., Goessler, W., Francesconi, K.A., 2008.  
623 Natural variability and distribution of trace elements in marine organisms from Antarctic  
624 coastal environments. *Antarct. Sci.* 20, 39–51. doi:10.1017/S0954102007000831

625 Ianni, C., Magi, E., Soggia, F., Rivaro, P., Frache, R., 2010. Trace metal speciation in coastal and  
626 off-shore sediments from Ross Sea (Antarctica). *Microchem. J.* 96, 203–212.  
627 doi:10.1016/j.microc.2009.07.016

628 Illuminati, S., Annibaldi, A., Romagnoli, T., Libani, G., Antonucci, M., Scarponi, G., Totti, C., Truzzi,  
629 C., 2017. Distribution of Cd, Pb and Cu between dissolved fraction, inorganic particulate and  
630 phytoplankton in seawater of Terra Nova Bay (Ross Sea, Antarctica) during austral summer  
631 2011–12. *Chemosphere* 185, 1122–1135. doi:10.1016/j.chemosphere.2017.07.087

632 Kahle, J., Zauke, G.-P., 2003. Trace metals in Antarctic copepods from the Weddell Sea  
633 (Antarctica). *Chemosphere* 51, 409–17. doi:10.1016/S0045-6535(02)00855-X

634 Kennedy, H., Thomas, D.N., Kattner, G., Haas, C., Dieckmann, G.S., 2002. Particulate organic  
635 matter in Antarctic summer sea ice: Concentration and stable isotopic composition. *Mar. Ecol.*  
636 *Prog. Ser.* 238, 1–13. doi:10.3354/meps238001

637 La Mesa, M., Eastman, J.T., Vacchi, M., 2004. The role of notothenioid fish in the food web of the  
638 Ross Sea shelf waters: A review. *Polar Biol.* 27, 321–338. doi:10.1007/s00300-004-0599-z

639 Majer, A.P., Petti, M.Â.A.V., Corbisier, T.N., Ribeiro, A.P., Theophilo, C.Y.S., Ferreira, P.A. de L.,  
640 Figueira, R.C.L., 2014. Bioaccumulation of potentially toxic trace elements in benthic  
641 organisms of Admiralty Bay (King George Island, Antarctica). *Mar. Pollut. Bull.* 79, 321–325.  
642 doi:10.1016/j.marpolbul.2013.12.015

643 Mäkelä, A., Witte, U., Archambault, P., 2017. Ice algae versus phytoplankton: Resource utilization  
644 by Arctic deep sea macroinfauna revealed through isotope labelling experiments. *Mar. Ecol.*



645 Prog. Ser. 572, 1–18. doi:10.3354/meps12157

646 Mancinelli, G., Vizzini, S., Mazzola, A., Maci, S., Basset, A., 2013. Cross-validation of  $\delta^{15}\text{N}$  and  
647 FishBase estimates of fish trophic position in a Mediterranean lagoon: The importance of the  
648 isotopic baseline. *Estuar. Coast. Shelf Sci.* 135, 77–85. doi:10.1016/j.ecss.2013.04.004

649 McMeans, B., Rooney, N., Arts, M., Fisk, A., 2013. Food web structure of a coastal Arctic marine  
650 ecosystem and implications for stability. *Mar. Ecol. Prog. Ser.* 482, 17–28.  
651 doi:10.3354/meps10278

652 Morata, N., Poulin, M., Renaud, P.E., 2011. A multiple biomarker approach to tracking the fate of  
653 an ice algal bloom to the sea floor. *Polar Biol.* 34, 101–112. doi:10.1007/s00300-010-0863-3

654 Negri, A., Burns, K., Boyle, S., Brinkman, D., Webster, N., 2006. Contamination in sediments,  
655 bivalves and sponges of McMurdo Sound, Antarctica. *Environ. Pollut.* 143, 456–67.  
656 doi:10.1016/j.envpol.2005.12.005

657 Nfon, E., Cousins, I.T., Järvinen, O., Mukherjee, A.B., Verta, M., Broman, D., 2009.  
658 Trophodynamics of mercury and other trace elements in a pelagic food chain from the Baltic  
659 Sea. *Sci. Total Environ.* 407, 6267–6274. doi:10.1016/j.scitotenv.2009.08.032

660 Norkko, A., Thrush, S.F., Cummings, V.J., Gibbs, M.M., Andrew, N.L., Norkko, J., Schwarz, A.M.,  
661 2007. Trophic Structure of Coastal Antarctic Food Webs Associated With Changes in Sea Ice  
662 and Food Supply. *Ecology* 88, 2810–2820. doi:10.1890/06-1396.1

663 Nygård, T., Lie, E., Steinnes, E., 2001. Metal dynamics in an Antarctic food chain. *Mar. Pollut. Bull.*  
664 42, 598–602. doi:10.1016/S0025-326X(00)00206-X

665 Petrou, K., Kranz, S.A., Trimborn, S., Hassler, C.S., Blanco Ameijeiras, S., Sackett, O., Ralph,  
666 P.J., Davidson, A.T., 2016. Southern Ocean phytoplankton physiology in a changing climate.  
667 *J. Plant Physiol.* 203, 135–150. doi:10.1016/j.jplph.2016.05.004

668 Post, D.M., 2002. Using Stable Isotopes to Estimate Trophic Position: Models, Methods, and  
669 Assumptions. *Ecology* 83, 703–718. doi:10.2307/3071875

670 Post, D.M., Layman, C.A., Arrington, D.A., Takimoto, G., Quattrochi, J., Montaña, C.G., 2007.  
671 Getting to the fat of the matter: Models, methods and assumptions for dealing with lipids in  
672 stable isotope analyses. *Oecologia* 152, 179–189. doi:10.1007/s00442-006-0630-x

673 Post, E., Bhatt, U.S., Bitz, C.M., Brodie, J.F., Fulton, T.L., Hebblewhite, M., Kerby, J., Kutz, S.J.,  
674 Stirling, I., Walker, D.A., 2013. Ecological Consequences of Sea-Ice Decline. *Science* (80-. ).  
675 341, 519–525. doi:10.1126/science.1235225

676 Prendez, M., Carrasco, M.A., 2003. Elemental composition of surface waters in the Antarctic  
677 Peninsula and interactions with the environment. *Environ. Geochem. Health* 25, 347–363.  
678 doi:10.1023/A:1024559809076

679 Rossi, L., di Lascio, A., Carlino, P., Calizza, E., Costantini, M.L., 2015. Predator and detritivore  
680 niche width helps to explain biocomplexity of experimental detritus-based food webs in four  
681 aquatic and terrestrial ecosystems. *Ecol. Complex.* 23, 14–24.  
682 doi:10.1016/j.ecocom.2015.04.005

683 Runcie, J.W., Riddle, M.J., 2004. Metal concentrations in macroalgae from East Antarctica. *Mar.*  
684 *Pollut. Bull.* 49, 1114–9. doi:10.1016/j.marpolbul.2004.09.001

685 Sañudo-Wilhelmy, S.A., Olsen, K.A., Scelfo, J.M., Foster, T.D., Flegal, A.R., 2002. Trace metal  
686 distributions off the Antarctic Peninsula in the Weddell Sea. *Mar. Chem.* 77, 157–170.  
687 doi:10.1016/S0304-4203(01)00084-6

688 Signa, G., Mazzola, A., Di Leonardo, R., Vizzini, S., 2017a. Element-specific behaviour and  
689 sediment properties modulate transfer and bioaccumulation of trace elements in a highly-  
690 contaminated area (Augusta Bay, Central Mediterranean Sea). *Chemosphere* 187, 230–239.  
691 doi:10.1016/j.chemosphere.2017.08.099

692 Signa, G., Mazzola, A., Kairo, J., Vizzini, S., 2017b. Small-scale variability in geomorphological  
693 settings influences mangrove-derived organic matter export in a tropical bay. *Biogeosciences*  
694 14, 617–629. doi:10.5194/bg-14-617-2017

695 Signa, G., Mazzola, A., Tramati, C.D., Vizzini, S., 2017c. Diet and habitat use influence Hg and Cd  
696 transfer to fish and consequent biomagnification in a highly contaminated area: Augusta Bay  
697 (Mediterranean Sea). *Environ. Pollut.* 230, 394–404. doi:10.1016/j.envpol.2017.06.027

698 Signa, G., Tramati, C., Vizzini, S., 2013. Contamination by trace metals and their trophic transfer to  
699 the biota in a Mediterranean coastal system affected by gull guano. *Mar. Ecol. Prog. Ser.* 479,  
700 13–24. doi:10.3354/meps10210

701 Tamelander, T., Reigstad, M., Hop, H., Carroll, M.L., Wassmann, P., 2008. Pelagic and sympagic  
702 contribution of organic matter to zooplankton and vertical export in the Barents Sea marginal  
703 ice zone. *Deep. Res. Part II Top. Stud. Oceanogr.* 55, 2330–2339.  
704 doi:10.1016/j.dsr2.2008.05.019

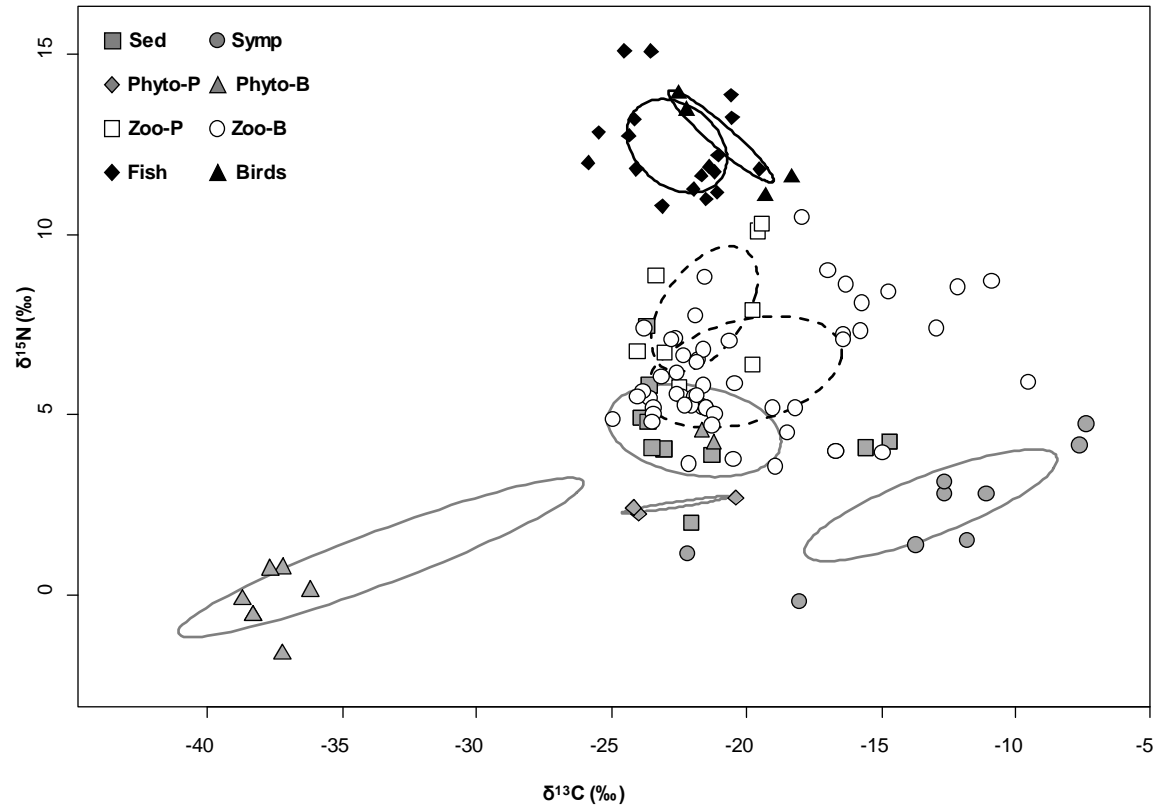
705 Trevizani, T.H., Figueira, R.C.L., Ribeiro, A.P., Theophilo, C.Y.S., Majer, A.P., Petti, M.A.V.,  
706 Corbisier, T.N., Montone, R.C., 2016. Bioaccumulation of heavy metals in marine organisms  
707 and sediments from Admiralty Bay, King George Island, Antarctica. *Mar. Pollut. Bull.* 106,  
708 366–371. doi:10.1016/j.marpolbul.2016.02.056

709 Tuohy, A., Bertler, N., Neff, P., Edwards, R., Emanuelsson, D., Beers, T., Mayewski, P., 2015.  
710 Transport and deposition of heavy metals in the Ross Sea Region, Antarctica. *J. Geophys.*  
711 *Res. Atmos.* 120, 10,996-11,011. doi:10.1002/2015JD023293

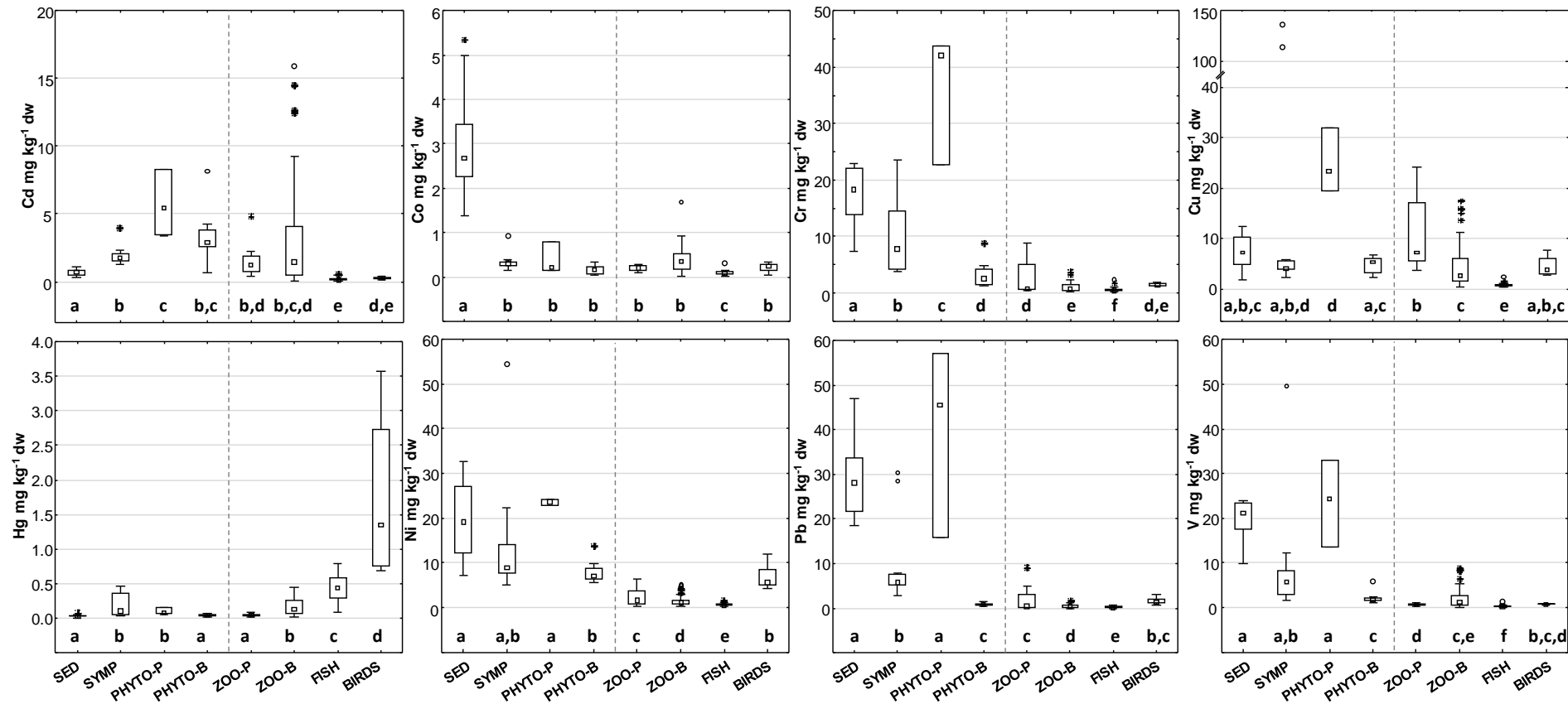
712 Vizzini, S., Signa, G., Mazzola, A., 2016. Guano-Derived Nutrient Subsidies Drive Food Web  
713 Structure in Coastal Ponds. *PLoS One* 11, e0151018. doi:10.1371/journal.pone.0151018

714 Wing, S.R., McLeod, R.J., Leichter, J.J., Frew, R.D., Lamare, M.D., 2012. Sea ice microbial  
715 production supports Ross Sea benthic communities: Influence of a small but stable subsidy.  
716 *Ecology* 93, 314–323. doi:10.1890/11-0996.1

717



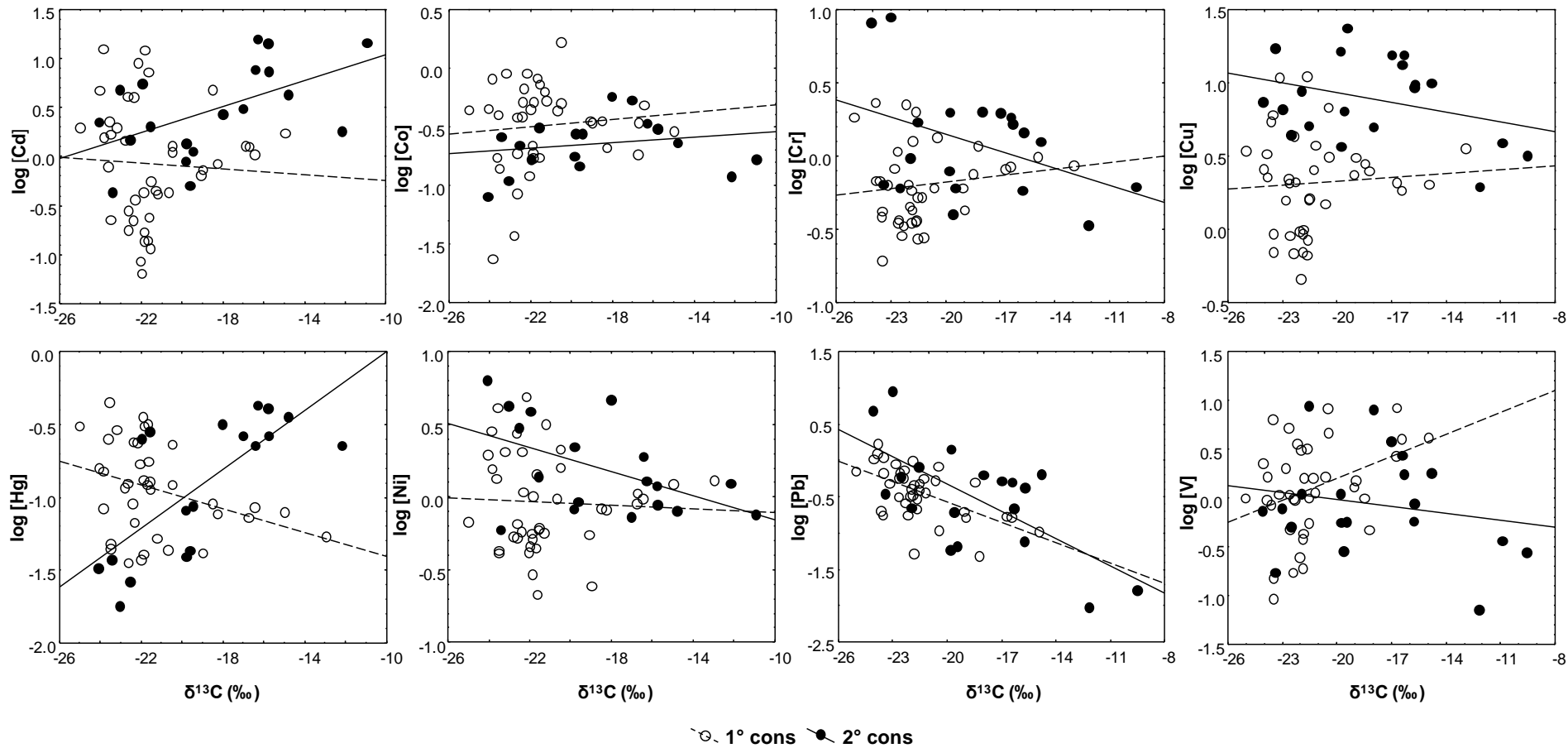
721 Fig. 1. Isotopic distributions of different basal sources (grey symbols), invertebrate (white symbols) and vertebrate (black symbols) taxa at Tethys  
722 Bay, Ross Sea (Antarctica). Different symbols represent different categories and each symbol represents a specimen. Ellipses encompass the  
723 core (i.e. 46%) of each categories.



724

725 Fig. 2. Trace element concentrations (mg kg<sup>-1</sup> dw) in organic matter sources: sediment organic matter (SED); sympagic algae (SYMP);  
 726 phytoplankton (PHYTO-P) and phytobenthos (PHYTO-B), and in consumers: zooplankton (ZOO-P); zoobenthos (ZOO-B); fish (FISH) and birds  
 727 (BIRDS) from Tethys Bay, Ross Sea (Antarctica). Whiskers indicate the non-outlier range of variation; boxes: 25th to 75th percentiles. Significant  
 728 differences among sample categories are indicated with different letters.

729



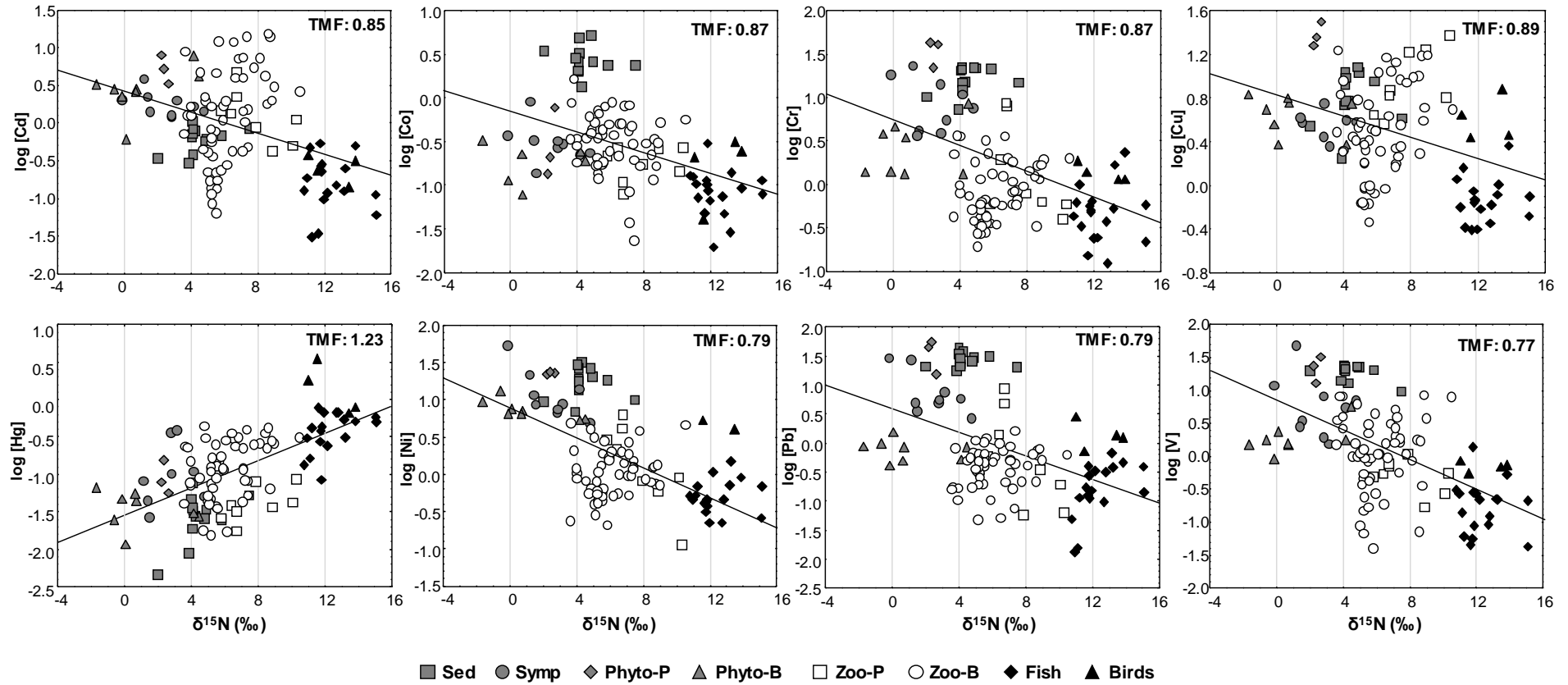
730

731 Fig. 3. Linear regressions for log-transformed trace element (TE) concentrations ( $\text{mg kg}^{-1} \text{ dw}$ ) vs.  $\delta^{13}\text{C}$  (‰) signatures of primary consumers in  
 732 white, and secondary consumers in black from Tethys Bay, Ross Sea (Antarctica). Regression equations and parameters ( $r$  and  $p$ -values) are  
 733 reported in Table 1.

734

735

736



737

738 Fig. 4. Linear regressions for log-transformed trace element (TE) concentrations ( $\text{mg kg}^{-1}$  dw) vs.  $\delta^{15}\text{N}$  (‰) signatures of the whole food web of  
739 Tethys Bay, Ross Sea (Antarctica). Trophic magnification factors (TMFs) are reported on each panel. Regression equations and parameters ( $r$  and  
740  $p$ -values) are reported in Table 1.

741 **Tables**

742 Table 1. Results of linear regressions (equation, coefficient of regression r and p value) between  
 743 log-transformed concentration of trace elements and stable isotopes:  $\delta^{13}\text{C}$  (primary and secondary  
 744 consumers) and  $\delta^{15}\text{N}$  (whole food web).

<b>a) <math>\delta^{13}\text{C}</math> vs. [log TE]</b>			
<b>Primary consumers</b>	<b>equation</b>	<b>r</b>	<b>p</b>
Cd	$y = -0.3849 - 0.0145*x$	-0.05	0.76
Co	$y = -0.1569 + 0.0156*x$	0.10	0.56
Cr	$y = 0.1152 + 0.0148*x$	0.14	0.40
Cu	$y = 0.5123 + 0.0091*x$	0.07	0.67
Hg	$y = -1.8228 - 0.0412*x$	-0.34	<b>0.04</b>
Ni	$y = -0.1618 - 0.0059*x$	-0.05	0.77
Pb	$y = -2.4367 - 0.0933*x$	-0.57	<b>0.00</b>
V	$y = 1.6903 + 0.0745*x$	0.36	<b>0.03</b>
<b>Secondary consumers</b>			
Cd	$y = 1.6931 + 0.0658*x$	0.53	<b>0.02</b>
Co	$y = -0.419 + 0.012*x$	0.20	0.42
Cr	$y = -0.6323 - 0.0391*x$	-0.40	0.09
Cu	$y = 0.4886 - 0.0223*x$	-0.32	0.16
Hg	$y = 1.0146 + 0.1012*x$	0.72	<b>0.00</b>
Ni	$y = -0.5732 - 0.0414*x$	-0.50	<b>0.03</b>
Pb	$y = -2.8261 - 0.1254*x$	-0.66	<b>0.00</b>
V	$y = -0.4854 - 0.0233*x$	-0.19	0.43
<b>b) <math>\delta^{15}\text{N}</math> vs. [log TE]</b>			
<b>whole food web</b>	<b>equation</b>	<b>r</b>	<b>p</b>
Cd	$y = 0.4271 - 0.0721*x$	-0.43	<b>0.00</b>
Co	$y = -0.419 + 0.012*x$	-0.46	<b>0.00</b>
Cr	$y = 0.7157 - 0.0814*x$	-0.48	<b>0.00</b>
Cu	$y = 0.8223 - 0.0493*x$	-0.38	<b>0.00</b>
Hg	$y = -1.5331 + 0.0897*x$	0.63	<b>0.00</b>
Ni	$y = 0.9326 - 0.1009*x$	-0.58	<b>0.00</b>
Pb	$y = 0.592 - 0.1016*x$	-0.46	<b>0.00</b>
V	$y = 0.8594 - 0.1139*x$	0.56	<b>0.00</b>

745